The Carbon-Water Interface: Modeling Challenges and Opportunities for the Water-Energy Nexus

Alberto Striolo,[1] Angelos Michaelides,[2] and Laurent Joly[3]

[1]Department of Chemical Engineering, University College London, London WC1E 7JE, United Kingdom; email: a.striolo@ucl.ac.uk

[2]Thomas Young Centre, London Centre for Nanotechnology, and Department of Physics and Astronomy, University College London, London WC1H 0AH, United Kingdom; email: angelos.michaelides@ucl.ac.uk

[3]Institut Lumière Matière, UMR5306 Université Lyon 1-CNRS, Université de Lyon, France; email: laurent.joly@univ-lyon1.fr

Annu. Rev. Chem. Biomol. Eng. 2016. 7:533–56

First published online as a Review in Advance on April 6, 2016

The *Annual Review of Chemical and Biomolecular Engineering* is online at chembioeng.annualreviews.org

This article's doi: 10.1146/annurev-chembioeng-080615-034455

Keywords

water desalination, carbon nanomaterials, reverse osmosis, capacitive deionization, force fields, ab initio

Abstract

Providing clean water and sufficient affordable energy to all without compromising the environment is a key priority in the scientific community. Many recent studies have focused on carbon-based devices in the hope of addressing this grand challenge, justifying and motivating detailed studies of water in contact with carbonaceous materials. Such studies are becoming increasingly important because of the miniaturization of newly proposed devices, with ubiquitous nanopores, large surface-to-volume ratio, and many, perhaps most of the water molecules in contact with a carbon-based surface. In this brief review, we discuss some recent advances obtained via simulations and experiments in the development of carbon-based materials for applications in water desalination. We suggest possible ways forward, with particular emphasis on the synergistic combination of experiments and simulations, with simulations now sometimes offering sufficient accuracy to provide fundamental insights. We also point the interested reader to recent works that complement our short summary on the state of the art of this important and fascinating field.

INTRODUCTION: THE IMPORTANCE OF REVERSE OSMOSIS IN WATER DESALINATION

The scientific community is facing the challenge of providing technological solutions for the water-energy nexus while preserving the environment. Carbon-based devices have been developed both for desalinating water and for storing energy. Such devices are characterized by vast carbon-water interfaces, owing to the ubiquity of nanopores. It is indeed possible that many, perhaps most water molecules within such devices come in contact with the carbon surface. Hence, a detailed understanding of water-carbon interfaces is necessary to ensure progress. Here, we review some recent advances obtained by atomistic simulations and experiments in this field.

Traditional water desalination approaches, such as multiflash distillations, are widely used but require large amounts of energy. As such, they are not sustainable in the long run. Reverse osmosis (RO) has become the technology of choice for most new installations. Two innovations are considered to be responsible for the wide application of RO: the introduction of thin-film composite membranes and the implementation of energy-recovery devices that reuse part of the energy present in pressurized brine (i.e., pressure exchangers and efficient pumps) (1, 2). Although RO is mature and reliable, it remains energy intensive (3–5). At its core are membranes permeable to water and impermeable to salt. The state-of-the-art membranes, based on polyamide thin-film composites, degrade in the presence of chlorine (which makes disinfection difficult) and are prone to fouling (6). Many believe that "in order for desalination to live up to the water challenges of the 21st century a step-change is needed in RO membrane technology" (7, p. 60). Although high mechanical strength as well as resistance to degradation and fouling are prerequisites to practical applications, much fundamental research seeks to identify nanostructured membranes that could yield high water fluxes and high salt rejection at the expense of limited pressure drops.

The remainder of this article is structured as follows: We first discuss some recent work related to the development of nanostructured membranes for water desalination, based either on carbon nanotubes (CNTs) or on graphene; we then propose a few ways forward, which we think could lead to the improvement of RO, as well as one alternative water desalination process (capacitive deionization, CD). Finally, we discuss how computer simulations could develop to continue to be relevant in this field. Rather than a comprehensive review, this is a brief, personal view on the subject. For other complementary perspectives, we refer the reader to previous discussions of emerging desalination technologies (5, 8–12) and nanofluidic transport (13–18).

CARBON NANOTUBE–BASED MEMBRANES

Among membranes likely to improve RO performance, those based on CNTs have attracted significant attention since early simulations showed that water molecules can travel extremely quickly through narrow CNTs (19), suggesting low drag losses (20). Considerable progress has been made, with experimental data in general consistent with the early simulations. Because CNTs are made of hydrophobic sp2-hydridized carbon atoms, the initial simulations reporting water adsorption inside CNTs attracted attention—sometimes even skepticism. To understand this puzzling result, the free energy changes for water as it enters CNTs of various diameters at ambient conditions were recently computed (21). The results show that the classical atomistic model of water known as single point charge extended (SPC/E) adsorbs spontaneously within CNTs with a diameter of 0.8–2.7 nm, but that the driving force depends on diameter (see **Figure 1**). For 0.8–1.0-nm CNTs, confined water is in a vapor-like phase stabilized by entropy, whereas water confined within 1.1–1.2-nm CNTs is ice-like, stabilized by enthalpy. Water confined in CNTs wider than 1.4 nm is liquid, in a bulk-like structure stabilized by large translational entropy. Many

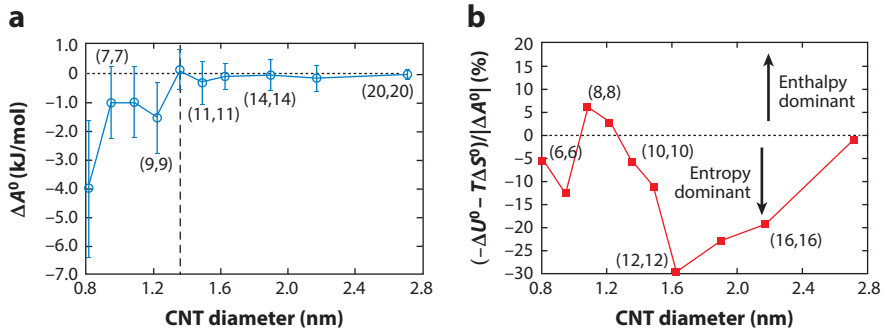

Figure 1

Changes in free energy for water molecules as they transfer from bulk liquid to the interior of infinite single-walled carbon nanotubes of varying diameter: simulations conducted at ambient conditions with the single point charge extended (SPC/E) model for water. The carbon nanotubes (CNTs) are labeled according to their chirality. (*a*) Relative Helmholtz free energy, ΔA^0 (confined water relative to bulk water). The dashed line indicates the convergence for bulk water. (*b*) Percentage of the free energy ΔA^0 arising from enthalpic (ΔU^0) or entropic (ΔS^0) contributions. The dashed line indicates conditions at which the two contributions cancel each other out. Figure reproduced with permission from Reference 19.

simulations also considered the transport of water inside CNTs (22). Among these, Striolo used molecular dynamics (MD) simulations to show that the fast water transport is due to the combination of strong water-water attractions and relatively weak and smooth CNT-water interactions (23). Falk et al. (24, 25) identified the crucial role of wall curvature in reducing water friction at the wall of CNTs. Joseph & Aluru (26) investigated the pressure-driven flow of liquid water through (16,16) CNTs of diameter 2.17 nm. They found an ~2,000× enhancement of mass flow rate with respect to that predicted by continuum theory, a consequence of the velocity jump in a region depleted of water at the water-CNT interface. Joseph & Aluru also showed that changes in the effective tube-water interactions, atomic-scale roughness of the CNT walls, and even small increases in the atomic carbon-carbon distance within the CNTs can decrease the water flow, further suggesting that the nanotube properties can manipulate the water transport. These results are consistent with others suggesting that even just a few defects, e.g., a few oxygenated sites (27) or constrictions along the tube axis (28), can affect the water flow through CNTs.

On the experimental front, Majumder et al. (29) fabricated membranes composed of aligned multiwalled CNTs of ~7-nm diameter, with area density of $\sim 5 \cdot 10^{10}$ per cm^2, crossing a polystyrene film. They measured water permeability, and they estimated the fluid velocities through the CNTs to be four to five orders of magnitude faster than those predicted by the Hagen-Poiseuille equation assuming laminar flow and zero velocity at the pore walls. They estimated a slip length from ~3 μm to 70 μm, much larger than the pore radius, and they reported that the fast water flow decreased after a few minutes. The interpretation of the fast water transport was consistent with the simulations discussed above [although the measured slip lengths were more than two orders of magnitude larger than the most favorable MD prediction (14)], whereas the decrease of flow over time was ascribed to a flow-induced solvent ordering. It was pointed out that the availability of a high density of pores allows for macroscopic measurements of fluid transport. However, Sisan & Lichter (31) suggested that difficulties in accurately determining channel radii, the number of channels spanning the membrane, and perhaps the net flow rates could yield inaccurate estimates of water flow rates through CNT membranes. In fact, when the pore properties are measured, different data for fluid transport are obtained. Using membranes with monodisperse

CNTs of inner diameter ~2 nm, Holt et al. (32) reported water flow rates two to four orders of magnitude faster than those predicted by continuum theories, but a few orders of magnitude smaller than those reported by Majumder et al. (29), and consistent with MD predictions (14). Experiments on individual CNTs of 0.81–1.59-nm diameter showed flow-enhancement rates below 1,000 (33), and sometimes just modest enhancements of water transport through individual CNTs (K.V. Agrawal, S. Shimizu, L.W. Drahushuk, D. Kilcoyne, and M.S. Strano, manuscript submitted). In summary, the experimental data are consistent in showing enhanced water flow through narrow CNTs, but the enhancement factor with respect to continuum fluid dynamics calculations is not uniquely determined.

One would expect that molecular simulations would help not only to identify the mechanism by which flow is enhanced but also to quantify the enhancement factor. Unfortunately, simulations have not been conclusive. We discuss below some of the inherent limitations in the accuracy of the classical models used in typical water-CNT simulations. Here we comment on the fact that very often simulations are conducted in periodic systems. In such cases potentially important pore-entrance and pore-exit effects are ignored (31). Joly (34) highlighted the crucial role of entrance effects in the capillary filling of a CNT with water using MD, and Gravelle et al. (35, 36) showed that using a conical entrance could minimize entrance dissipation. Walther et al. (37) conducted massive MD simulations to reproduce the experimental setup of Holt et al. (32) (i.e., double-walled CNTs spanning hydrophilic membranes 3–2,000 nm thick). Three stages were identified: (*a*) water entry and filling of the CNTs, (*b*) water emergence and droplet formation at the pore exit, and (*c*) water flow through the CNT connecting two water reservoirs. Under imposed pressures of ~1 bar, water entry and exit from the CNTs depended on the state of the membranes, with prewetted membranes allowing water to infiltrate the CNTs. Data analysis showed a slip length of ~63 nm, independent of the thickness of the membrane, and a significant entrance loss. Entrance losses were found to be the dominant losses for membranes of thickness three nm or less. Once the entry losses are accounted for, Walther et al. (37) showed that the flow rate increases linearly with the pressure gradient, which was not in agreement with the findings of Thomas & McGaughey (38), who reported nonlinear dependence but did not account for entrance losses. Walther et al. (37) estimated that entrance and exit effects could be ignored for CNT-based membranes with thickness of at least ~300 nm. Functionalizing the entrance of the CNT may affect these resistances: Majumder et al. (39) functionalized the CNT ends in their experimental membranes and reduced water permeability compared with unfunctionalized CNTs by three orders of magnitude; when they also functionalized the interior of the CNTs, the increase in water flux was only a factor of five compared with traditional expectations (29). The interpretation proposed for their experimental observations is that the functional groups affect the slip boundary condition.

We concentrate now on salt rejection. Thomas et al. (16) proposed six mechanisms to tailor salt rejection in nanoporous membranes: (*a*) size exclusion of the bare ion, (*b*) steric exclusion of the hydrated ion, (*c*) charge repulsion, (*d*) specific ion-pore interactions, (*e*) interactions between ions and chemical structures in the pore, and (*f*) entropic differences. By manipulating the CNT diameter, it is possible to maximize the first three of these criteria. The fourth criterion refers to subtle effects owing to the overall morphology of the pore, as suggested by biological pores (40, 41). A study inspired by structure-function properties of biological channels showed that it is possible to control the conduction of ions through a CNT compressed laterally (28). These simulations were conducted for aqueous electrolyte solutions containing KCl through (12,12) CNTs. Water, K^+, and Cl^- ions were able to flow through a pristine (12,12) CNT; when the central section of the CNT was compressed to form a conical constriction, first the ions were not allowed to flow through, and then neither water nor ions flowed. The blockage to ionic fluxes was due to the dehydration of the ions. This simulation suggests the possibility of tuning the conductivity of

nanostructured membranes using mechanical deformations, which could be reversible because of the CNTs' material properties.

GRAPHENE-BASED MEMBRANES

Because of graphene's mechanical strength, its imperviousness to atoms as small as helium, and optimistic atomistic simulation results (42–44), it is generally expected that nanoporous graphene with sufficiently high density of pores could yield ultrafast water permeance, because of the little resistance to flow expected by the atomic thinness of the membrane, and high salt rejection because the passage of solutes larger than the pores should be prevented (45). Note, however, that Gravelle et al. (36) showed, using MD simulations, that the permeability of a small CNT with conical entrances can exceed that of a graphene sheet pierced with a hole of similar size to the CNT diameter. Cohen-Tanugi & Grossman (7) reviewed computational studies on single-layer graphene for RO.

Assuming a pore density of $\sim 10^{13}$ nanopores per cm^2, Cohen-Tanugi & Grossman, using nonequilibrium MD simulations, estimated a permeability approximately two to three orders of magnitude larger than that observed in thin-film composite membranes. The results depended greatly on the nanopore size, and on the functional groups at the pore edges. The pores needed to be ~0.27 nm to reject salt effectively. Because the efficiency falls dramatically as the pore size increases to ~0.4 nm, to manufacture RO membranes, it is necessary to achieve extremely high accuracy in producing pores, and to ensure that the graphene sheets remain intact during operation. Konatham et al. (46) investigated, using equilibrium MD, how functionalizing the pores could help in rejecting salt ions. They reported the effective potential of mean force (PMF) for water, Na^+, and Cl^- ions through the pore. The narrow pores were decorated with chemical groups such as COO^- and OH. The PMF was calculated along the vertical distance from graphene, through the pore center. High free energy barriers when the molecules approached the pore were interpreted as signatures of effective rejection (i.e., high water permeability requires small free energy barriers). The results showed that if the pores are too narrow, steric effects prevent water from flowing through; if the pores are too wide, the functional groups are not sufficient to reject salt. When the pores are ~0.75 nm in diameter, functional groups can help: Charge effects are effective (i.e., COO^- groups yield high free energy barriers for Cl^- ions), but as the salt concentration increases, electrostatic repulsions are screened. It was encouraging to observe that OH groups remained effective at rejecting both Na^+ and Cl^- ions at 0.25 M. These results suggest that steric effects remain a dominant mechanism for salt exclusion at moderate salt concentrations.

Despite encouraging computational results, leakage has prevented the implementation of graphene-based RO experimental devices. To address this limitation, O'Hern et al. (47) produced a graphene layer and transferred it onto a porous polycarbonate membrane that provides structural support. The graphene shows 1–15-nm pores and large tears. The authors filled the tears using atomic layer deposition and repaired the nanometer-scale defects using Nylon 6,6. New 0.5-nm pores were introduced by ion bombardment, followed by etching (47). The membrane permeability was comparable to that of current RO membranes for seawater desalination (48). The membrane was tested with respect to the rejection of dextran (Mw 4.4 kDa), Allura Red (size ~1 nm), $MgSO_4$, and NaCl. The results were encouraging for dextran, Allura Red, and $MgSO_4$. Unfortunately, NaCl was found to permeate the membrane, possibly because it is able to diffuse through the Nylon 6,6 plugs. Because of the technical limitations just mentioned, and also because of the difficulty in generating pores well-controlled in size and chemical functionalization, it has so far been possible to conduct extensive experimentation only on single-layer graphene membranes of microscopic areas with a few pores (49–52). O'Hern et al. (47) reported

the synthesis of single-layer graphene membranes with pores that are uniform in size and whose chemical functionalization can be tailored. X-ray photoelectron spectroscopy measurements suggested the pores were terminated with ketone, quinone, hydroxyl, and/or carbonyl groups. The resultant membranes were tested toward their efficiency at repelling aqueous KCl and Allura Red. The permeability of both compounds increased using etching for 5 min, and if etching continued for longer than 25 min the membranes rejected only Allura Red, as the pores became too large to regulate ion transport. Although the membranes were not strong enough to be tested in pressure-driven RO experiments, the results suggest, in qualitative agreement with simulations, that it is possible to tune the pore properties, and doing so allows for regulation of the performance of graphene-based membranes.

As an alternative to single-layer graphene, many researchers are considering stacks of multiple graphene layers, after Nair et al. (53, p. 442) reported that graphene oxide (GO) membranes can be impermeable to helium and other gases, while allowing the "unimpeded permeation of water." GO membranes are easy to fabricate and mechanically robust, suggesting the possibility of large-scale production (54, 55). However, as Kim et al. (56) demonstrated, their performance depends on preparation. This group showed that selectivity to gas transport can be achieved by controlling the degree of interlocking between the GO sheets. Interlocking is expected to change the flow channels and the pore sizes. GO laminates were proposed for several applications, including CO_2 separation from gases (57) and RO (58, 59), and have been used for pressure-driven separations (59–62). Joshi et al. (63) reported on membranes prepared from GO suspensions using vacuum filtration. The manufactured membranes were vacuum-tight in the dry state but showed significant water flow rates when exposed to liquid aqueous solutions. Using different experimental techniques, Joshi et al. found that cations and anions moved through the membranes in stoichiometric amounts to maintain charge neutrality, and that the permeation rates were a strong function of the size of the hydrated ions, with species larger than ~0.45 nm effectively sieved out of the membrane. Atomistic MD simulations of graphene capillaries of width sufficient to allow the formation of one, two, and three layers of water molecules support their interpretation. Joshi et al. found that when the width of the pore allowed the formation of a single layer of water, no ions were able to penetrate the capillaries; the ions were able to penetrate the pores when two to three water layers were present, but any molecule larger than ~0.45 nm was excluded. The combined simulation/experiment results suggest that the permeation of the GO membranes is determined by regions within the pore network in which only two to three layers of water molecules are allowed. Therefore, understanding the structure and dynamics of aqueous solutions confined in narrow carbon-based pores is of tremendous importance. Many studied the adsorption and transport of water in carbon-based porous materials (64–66). For example, Striolo et al. (67, 68) investigated systematically the adsorption isotherms for water in carbon pores of different geometry and varying widths and in a wide temperature range.

For the present review, it is more important to point out how the simulation results help identify the structure of confined liquid water, often quantified in terms of density profiles. See, for example, in **Figure 2** how the pore width affects the layers of water. Understanding water confined in slit-shaped carbon pores is also relevant in understanding hydrophobic interactions (69–72). The length scale at which liquid water becomes unstable when confined between hydrophobic plates has recently been quantified (73–75), as well as the molecular pathways that lead to dewetting (76). Bakli & Chakraborty (77) used MD to assess whether the presence of salts affects the hydrodynamics of water confined in slit channels, with the water-solid interactions chosen to reproduce wetting and nonwetting conditions (monitored by the sessile contact angle). They observed a direct relationship between contact angle and slip length, with no slip in the wetting channel and some slip in the nonwetting one. They then observed that when salt was added to the wetting system, the slip length

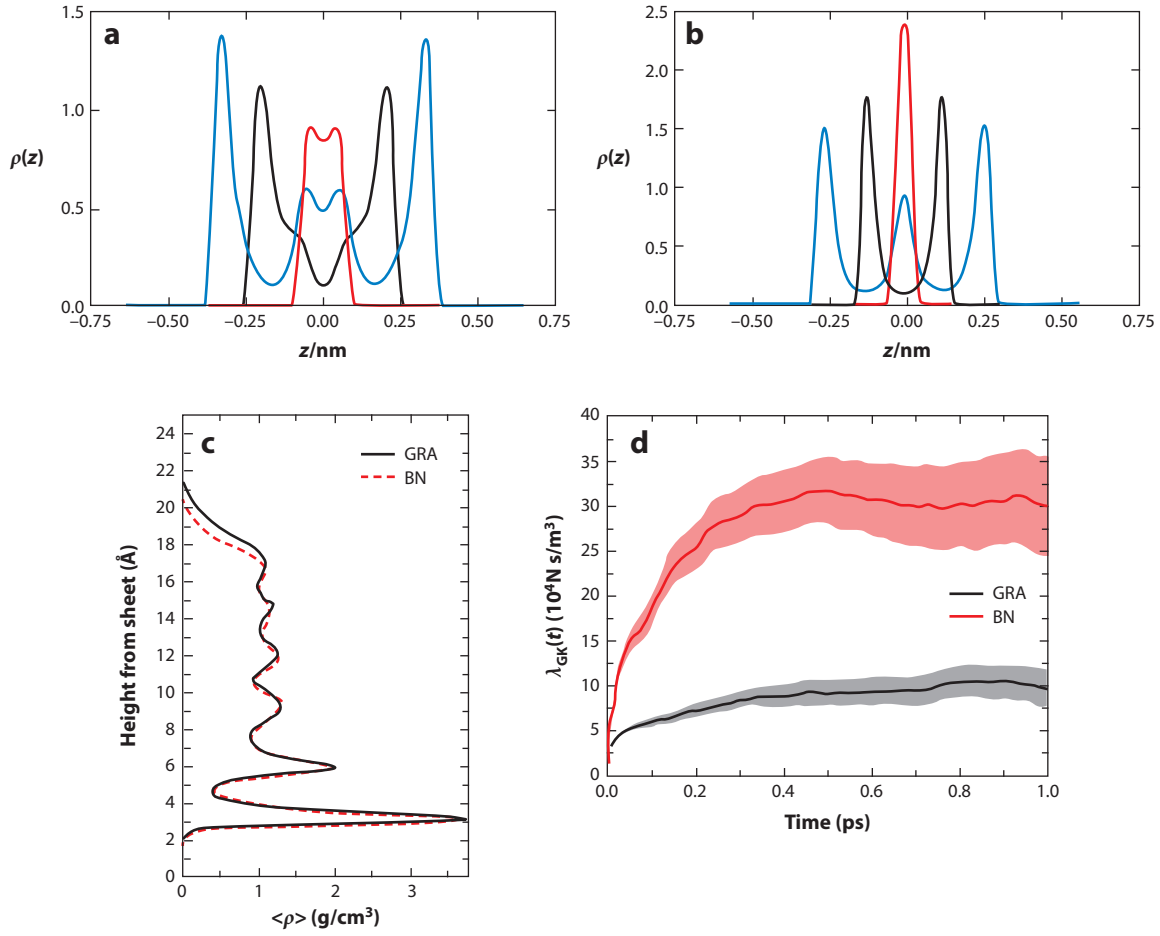

Figure 2

(*a*,*b*) Density profiles of the oxygen atom of water confined within carbon-slit pores of varying width; these simulations were conducted for the single point charge extended (SPC/E) model of water, using the grand canonical Monte Carlo algorithm at 298 K and at conditions at which the pores just filled with liquid water; blue, black, and red lines are for pores of different widths: 1.30, 1.05, and 0.75 nm in *a* and 1.15, 0.85, and 0.65 nm in *b*, respectively. (*c*) Structure of a liquid water film on graphene (GRA) and a single sheet of hexagonal boron nitride (BN). Specifically, the average density profile $\langle\rho\rangle$ as a function of the height from the sheet is shown. The liquid film structure is essentially the same on both sheets (on BN, the film is slightly thinner because the BN unit cell is slightly larger than that of graphene). (*d*) Comparison between the Green–Kubo estimate of the friction coefficient of liquid water on GRA and on BN. The shaded areas represent the uncertainties obtained by performing a block average. The friction coefficient λ is given by the plateau value at long times. There is an evident increase in the friction coefficient on BN. Figures adapted with permission from Reference 67 and Reference 82, ©2003 and 2014 American Chemical Society.

increased, whereas when salt was added to the nonwetting system, the slip length decreased. The slip length correlated with the maximum in molecular density within the first hydration layer, consistent with the analysis of slip length by Barrat & Bocquet (78). Bakli & Chakraborty (77) also found evidence of salt-specific effects related to the ion hydration strength and extended their investigation to electrokinetic energy conversion (79). Joly et al. (80) investigated the effect of salt on slip length with charged confining walls. In that case, the slip length was mainly controlled by the surface charge, and salt concentration effects were negligible.

Several of the studies discussed so far were concerned with the hydrodynamic boundary condition used to describe water flow. Recently, Ho et al. (81) challenged the traditional view according to which hydrodynamic slip can occur only for water on surfaces that are hydrophobic. They used nonequilibrium MD to quantify the hydrodynamic slip length on materials that, based on the water contact angle, could be classified as either hydrophobic (graphene) or hydrophilic (materials inspired by magnesium oxide). The results showed evidence for hydrodynamic slip on graphene, as expected (24), but also on some of the hydrophilic materials. The key ingredient for hydrodynamic slip to occur was that the interfacial water molecules should be able to move from one preferential adsorption site to a neighboring one without necessarily desorbing from the first hydration layer. Tocci et al. (82) investigated hydrodynamic slip of liquid water on graphene and, for comparison, a single layer of hexagonal boron nitride (BN) using equilibrium ab initio MD (AIMD), with forces obtained on the fly from electronic structure calculations. Green-Kubo relations were used to extract friction coefficients (83, 84). It was found that although the structures of the liquid water film on the two surfaces were exceedingly similar, the friction coefficient on BN was approximately three times larger than that on graphene (see **Figure 2**), because of the greater corrugation of the energy landscape on BN. This result arose from specific electronic structure effects and revealed a subtle dependence of the friction on the atomistic details of a surface, which is not directly related to its wetting properties. To ensure progress in GO membranes, it should be investigated how oxygenated groups could affect results such as those just described, both in terms of the structure and dynamics of confined water and in terms of its tendency to dewet the pores. In fact, the presence of a few groups that favorably interact with water on an otherwise hydrophobic surface strongly affects both the structure of interfacial water (27, 85, 86) and the tendency of water to evacuate confined regions (87–89, 89a).

RESEARCH NEEDS TO ADVANCE WATER DESALINATION VIA REVERSE OSMOSIS

To further develop CNT-based and graphene-based membranes, a synergistic combination of theoretical and experimental studies on single-pore systems is needed. Along these lines, Bocquet and coworkers (90) developed instruments capable of probing extremely small mass transport across individual nanochannels by adapting the Coulter technique (the electrical resistance across a channel increases when a large compound, e.g., a salt ion, crosses the channel because it reduces the amount of water within the channel). Using statistical analysis of measured current as a function of time, they measured water flows with an accuracy of a few femtoliters per second, two orders of magnitude better than state-of-the-art methods. Strano and coworkers (91) investigated individual, isolated CNTs. In particular, they monitored the electroosmotic current through the CNT interior, observing stochastic pore blocking when individual cations partitioned into the CNT. Recently, Strano and coworkers (K.V. Agrawal, S. Shimizu, L.W. Drahushuk, D. Kilcoyne, and M.S. Strano, manuscript submitted) measured, using two complementary techniques, the diameter-dependent liquid-solid phase boundaries for water within CNTs 1.05, 1.06, 1.15, 1.24, and 1.52 nm in diameter. They analyzed the radial breathing mode of the CNTs as they were filled with water and measured water transport at various temperatures. The results show both an exquisite sensitivity to diameter and substantially larger temperature elevations of the melting transition than theoretically predicted. Reversible melting was observed at 138°C and 102°C for water in 1.05-nm and 10.6-nm CNTs, respectively. A near-ambient phase change at 15°C was observed in 1.52-nm CNTs, whereas inside 1.24-nm CNTs freezing was suppressed below −30°C. This is interesting from a fundamental point of view, because fluid phase transitions inside single, isolated CNTs are predicted to deviate substantially from bulk ones (92), and also from

a practical point of view, because CNT-based membranes would cease to function if the water confined within the individual pores were to solidify.

The availability of single-pore platforms could allow the generalization of the proof-of-concept results reported by Majumder et al. (93), who took advantage of the possibility of functionalizing the ends of the CNTs embedded in a membrane to control, via applied voltages, the transport of ruthenium bipyridine hexahydrate. These data suggest that the transport selectivity of advanced nanostructured membranes can be achieved by taking advantage of functionalization. Experimental data are available for a single pore drilled in graphene because of the potential application of such devices in DNA sequencing applications (26, 28). For example, Garaj et al. (50) used chemical vapor deposition (94, 95) to produce $0.5 \cdot 0.5$ mm^2 graphene membranes mounted on a free-standing SiN_x layer. They found a linear relationship between the ionic conductivity across the membranes with one single pore, created using electron beam drilling, and the pore diameter. These results suggest that the effective insulating thickness of the graphene membrane is ~0.6 nm, consistent with atomistic MD simulations (96), which indicate that the distance between water and carbon atoms on both sides of a layer of graphene is ~0.3 nm (see **Figure 2**). The linear relationship between ionic conductivity and pore diameter, rather than pore area, is expected for atomically short nanopores in which the resistance is dominated by the access resistance (97), and it is consistent with the solution of the Laplace equation across idealized uncharged insulating membranes. The experimental data were initially obtained for ~5-nm-diameter pores (50), and more recently for pores as small as ~3 nm (51). Although these results are impressive, for the development of RO membranes it would be beneficial to push their limits to test subnanometer pores, with a high degree of control also on the chemical functionalization of the pore edges. Such data would be directly comparable to simulation results.

Although most of the research summarized above aims to improve RO membranes, it should also be pointed out that additional reductions in the pressure drop across a membrane might not yield the expected improvement in practice. Thermodynamics is the culprit, as the difference in osmotic pressure between purified and salty water will always cause a pressure drop across the membrane. Several researchers estimated the benefits, in terms of overall energy consumption, that can be expected from new membranes. Considering that in practical water desalination operations the salt rejection across a RO membrane is ~99% or higher (98), the minimum hydraulic pressure required to generate desalinated water from a brine solution will have to be larger than the osmotic pressure difference between permeate and retentate solutions. The pressure drop across the membrane will be added to this minimum. The state of the art in RO has reached energy efficiencies that are not considered too far from the thermodynamic limit of a single-stage operation (in a single-stage operation, salty water is fed to the separation, the retentate is the more concentrated solution to be disposed of, and the permeate is the desalinated water) (99). Scientists wonder what more can be achieved with expensive nanostructured membranes. Perhaps better energy efficiency can be achieved by changing the configuration of the desalination processes. Lin & Elimelech (100) recently compared the energy requirements in multistage processes, either in direct pass or in closed-circuit realizations, and quantified their benefits compared with single-stage processes. Others remain convinced that "graphene holds promise as an ultimate RO membrane" and suggest that new nanostructured membranes resistant to chemical degradation can be obtained using graphene (7, p. 60). Cohen-Tanugi et al. (7, 101) modeled the performance of a RO plant, taking into consideration feed salinity and flow rate, concentration polarization across the membrane, membrane permeability, and a few other key parameters, although they omitted the effect of fouling. Their calculations suggested that a membrane three times more permeable than existing ones could reduce the pressure required for seawater treatment by 15%.

However, they also pointed out that new membranes 1,000 times more permeable than the current ones would not lead to great improvements in energy efficiency (7, 101).

Regarding fouling, Belfort and his group (102, 103) recently proposed an experimental combinatorial method for synthesizing, screening, and discovering antifouling surfaces. This group developed a high-throughput platform that employs atmospheric-pressure plasma polymerization to modify commercial poly(ether sulfone) membranes. They investigated the effect of carbon chain length of the functional groups and found that a minimal chain length of four to six carbons is required for hydroxyl and poly(ethylene glycol) monomers to achieve antifouling. When the chains are shorter or longer, the performance decreases (103). More recently, they quantified the effect of new functional graft-polymerized groups. They quantified performance in terms of fouling index, solute selectivity, and flux (103). To rationalize the results, they calculated the Hansen solubility parameter (104) of the synthesized monomers and found that the best-performing membranes had functional groups whose Hansen solubility parameter was closest to that of water. Although this pragmatic observation is useful for securing progress, it suggests that local properties, in particular water-monomer interactions, are responsible for rather large-scale phenomena, such as protein adsorption (105). Many studies have been conducted on water properties at the interface with solid substrates (106, 107), and perhaps the most intriguing breakthroughs from recent discoveries are the correlation between water density fluctuations near an interface and the ability of various macromolecules to adsorb (108) and perhaps even the solubility of gases in confined water (109, 110). The latter studies suggest that the proximity of two surfaces affects not only the structure and dynamics of confined water but also the ability of water molecules to fluctuate. By extension, it would be interesting to determine how the proximity of functional groups affects water properties at an interface, and how these effects are related to data such as those presented by Belfort and coworkers.

ALTERNATIVE WATER DESALINATION PROCESSES: CAPACITIVE DEIONIZATION

An alternative approach to desalinate water is capacitive deionization, CD (111, 112). The process came back to the spotlight recently with the enhanced interest in electric double-layer capacitors (EDLCs) for energy storage (113). Both CD and EDLCs work via the accumulation of ions at charged electrode-electrolyte interfaces (114). CD can be attractive compared with RO because its goal is to collect ions from salty water, rather than process all water molecules through membranes. Because the amount of ions that can be captured using CD scales with the electrode's surface area, conductive porous materials such as active carbons with high surface area are used (115, 116). Challenges to bringing CD to fruition include the maximization of the capacitance, to capture more ions, and synchronization of water flow through the device (117). In fact, once ions are adsorbed on the electrodes, the latter need to be regenerated (118), making CD processes discontinuous, unless complicated operations are designed [e.g., desalination with wires (119)].

Recently, the community has made significant strides that can benefit CD. In particular, the energy barriers encountered by different ions as they enter narrow carbon-based pores from bulk solutions were quantified (120–122), as well as ion-ion and ion-water correlations under confinement (123–125). Kalluri et al. (126) reported a combination of electrochemical experiments, supported by atomistic simulations, to quantify the effects of pore size and surface charge density on the capacitance of graphitic nanoporous carbon electrodes. Carbon foams were produced with two distinct pore size distributions (nonactivated materials characterized by subnanometer pores and activated ones with pores as wide as ~2 nm). The cyclic voltammetry data obtained for the activated pores showed ideal (linear) capacitive behavior (i.e., rectangular shape and charging/discharging

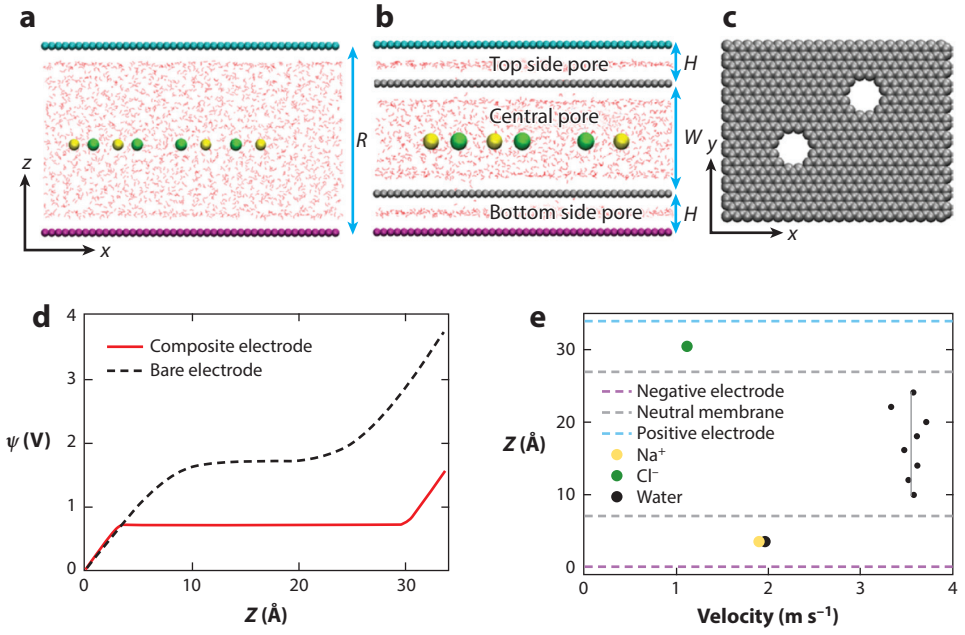

Figure 3

(*a–c*) Schematic of simulated water desalination cells. (*a*,*b*) Side views of two cells: the bare one, in which the positive and negative electrodes (*cyan* and *purple*, respectively) face across the pore volume, and the composite one, in which graphene membranes (*c*) are used to separate the central pore from top and bottom side pores. (*d*) The electrical potential profiles are calculated along the direction perpendicular to the electrode surface for bare and composite electrodes. (*e*) The steady-state velocities calculated for water molecules and ions within the composite electrode are reported as a function of the position within the composite cell. Adapted with permission from Reference 129, ©2015 American Chemical Society.

currents independent of the applied potential window), whereas the correspondent data obtained for the nonactivated pores showed strong increases in capacitance (>1 order of magnitude) when wide potential sweeps were applied. The latter results depend on the ions present in solution, with the peak that marked the transition from low to high capacitance shifting to more negative potentials as the strength of the hydration shell increased (no obvious correlation was found with the size of the ions or the size of the hydrated ions). These data were consistent with simulation results for the free energy barriers experienced by ions entering negatively charged CNTs (121), as well as with simulations reporting the density of ions confined within carbon slit-shaped pores at different surface charge densities (123, 127).

Ho & Striolo (128), using equilibrium MD simulations, found that the structure and orientation of interfacial water, as well as the accumulation of NaCl ions near the interface, depend on electrode patterning (the electrodes were graphene layers, patterned by removing selected carbon atoms). These effects led to significant variations in the capacitance of the electrodes. Ho & Striolo (129) also recently proposed, in another computational effort, to combine some features of membrane desalination and some of CD to obtain a continuous desalination device. In the proposed composite cell (see **Figure 3**), the charged electrodes extract the ions from the feed-water. The noncharged graphitic membranes manipulate the electric double layer and prevent the ions, once captured, from returning to the central pore. The resultant short distance between captured ions and charged electrodes increases the capacitance; in addition, water slips at the walls of the slit-shaped

channels (24), which allows for continuum operation. Based on these simulations, the cell could be operated continuously; could achieve 100% charge efficiency and recover 70% of the water initially loaded to the system with 100% salt rejection at salinity less than 10 g/L; and is expected to yield 30 L of desalinated water per cm^2 of membrane, per day, per MPa of pressure drop (129). Of course, experimental investigations are needed to bring this device to practical fruition, and to provide more realistic quantifications of the promising indicators just summarized.

FRONTIERS OF SIMULATION STUDIES

Although atomistic simulations have contributed to many areas of scientific endeavor, such as the development of solar cells (130), batteries (131), and new catalysts (132, 133), to name just a few, one must recognize that computational approaches have several limitations. Four key restrictions relate to (*a*) the accuracy of the potential energy surfaces, (*b*) the algorithms and sampling techniques used, (*c*) the description of the material, and (*d*) the finiteness of computational resources. We now briefly discuss how such limitations can be overcome to benefit water desalination.

Accuracy of the Potential Energy Surfaces

In all simulation studies, one must ensure that the theoretical approach used can faithfully describe the systems being considered. Most simulations discussed so far have been performed with empirical potentials (i.e., classical force fields), which are sensitive to the choice of the parameters used. Many classical models are available for the description of water-water interactions (134, 135), and some have been used to investigate interfacial systems (106).

Ho & Striolo (136) compared the predictions obtained by equilibrium MD simulations for water at contact with graphene. Among the models considered, it was found that the SPC/E, TIP4P/2005, SPC/Fw, TIP4P/2005f, and SWM4_DP models yielded structures of interfacial water on neutral, negatively, and positively charged graphene that were very similar to each other. Somewhat different predictions, in particular for the dynamics of interfacial water, were obtained when the TIP5P and the TIP3P models of water were considered. Liu & Patay (137) compared how different water models performed to predict water transport through CNTs. The fastest model (TIP3P) had a flow rate approximately five times greater than the slowest (TIP4P/2005), which was related to a different structure in confinement. Often, it is suggested that polarization effects, important to describe the water-vacuum interface (138), could be essential to reliably describe the graphene-water interface. Ho & Striolo (139) attempted to quantify effects owing to water polarizability on both structure and dynamics of water near graphene, neutral and charged. The results suggested that polarizability might not be important at the water-graphene interface. However, to judge which models are best at reproducing realistic scenarios, very detailed experimental information is required. Lacking this information, detailed ab initio simulations could yield important insights.

Besides water-water interactions, it could also be important to correctly describe carbon-carbon interactions. Once again, there are many carbon potentials of varying levels of sophistication to choose from. We do not discuss the details of the carbon potentials here except to mention two very recent force field studies for water in CNTs and on graphene, which have shown that the motion of the water can couple to the phonon modes of the graphene sheet or CNT (140, 141). This suggests that an accurate description of the phonon spectrum of the carbon material is a prerequisite for faithful predictions of water transport properties.

Once the models for water and carbon are chosen, one must consider the nature of the water-carbon interaction. Unfortunately, this is still not very well quantified, as adsorption energies of

isolated water molecules on well-defined surfaces are not well established (142). In the absence of better alternatives, the water-carbon interaction used in most studies was obtained by fitting to the macroscopic contact angle of water droplets (96). This approach has proved useful. However, given that the contact angle arises from a balance of surface energies, and because different water and carbon models yield different surface energies, the water-carbon interaction depends on the models used to describe water and carbon. Although this situation is not satisfactory, more troublesome is that the experimental contact angle for water droplets depends sensitively on experimental conditions (particularly impurities and defects) and is itself a matter of debate (143–145). Alternatively, the water-carbon interaction can be obtained directly from the electron density by using, for example, Kohn-Sham density functional theory (DFT) without relying on empirical parameters. DFT has been widely used to study water on carbonaceous surfaces (146–153).

However, practical DFT calculations do contain approximations, most notably in how electron exchange and correlation effects are treated within the so-called exchange-correlation (xc) functional. Nowadays, there is an almost endless list of xc functionals (154, 155), and especially for weak interaction systems, such as water adsorption on carbonaceous surfaces, the results can vary significantly from one functional to the next. **Figure 4** illustrates the predicted adsorption energy of a single water monomer on graphene as obtained from a variety of DFT xc functionals (as well as other ab initio methods). It can be seen that the predicted adsorption energies vary from ~150 meV (~4 kcal/mol) right down to nothing at all. Of course, the xc functionals that predict no binding are not appropriate for this system. The lack of any binding arises because the correspondent functionals do not account for van der Waals forces, an issue that DFT developers are addressing with vigor (156). Nonetheless, it is clear that at present one cannot easily turn to DFT for a benchmark of the water-carbon interaction. With this in mind, there have been several other studies using yet more sophisticated electronic structure theories aimed at establishing an accurate theoretical reference for the interaction of water with sp2-bonded carbon (146, 157–162). This has involved a very broad range of approaches, such as periodic quantum Monte Carlo, random phase approximation calculations, coupled cluster, and symmetry adapted perturbation theory on acene clusters. Wu & Aluru (157) tabulated many of the results, and although a consensus has yet to be reached, these high-level calculations yield values in the 70–120-meV range (~2–4 kcal/mol).

In desalination studies, it is necessary to also describe ion-water and ion-ion interactions. With regard to this issue, it is important to point out that the community has recently realized that widely used classical force fields might not be sufficiently accurate to describe the solubility of salt in water, because they were parameterized to reproduce properties of individual salts (163, 164). Ding et al. (165) compared the predictions of force field and AIMD for the self-diffusion of water in the presence of NaCl and CsI salts. They suggested that only ab initio simulations can reproduce the qualitative trends observed experimentally (166). They then showed that the anomalous water diffusion in salt solutions has a subtle origin involving electronic properties of water. Classical force fields cannot easily describe such effects, which can, of course, be captured by ab initio methods. Although this might not be a significant limitation when single ions are considered, it could compromise the reliability of the simulation predictions when one is interested in simulating the accumulation of ions within a charged carbon-based pore (of relevance in CD) and when one is interested in quantifying concentration effects (i.e., screening) on ion rejection. We refer the interested reader to a recent contribution by Jiang et al. (167), who found that for aqueous systems containing NaCl the polarizable force field of Kiss & Baranyai (168) yields much better predictions for quantities such as salt solubility, solution density, and viscosity as a function of system temperature, pressure, and salt concentration than fixed-point nonpolarizable models do.

DFT approaches have been employed to better understand ion-water interactions, and in particular the hydration shell. For a brief review of DFT studies of aqueous solutions, the

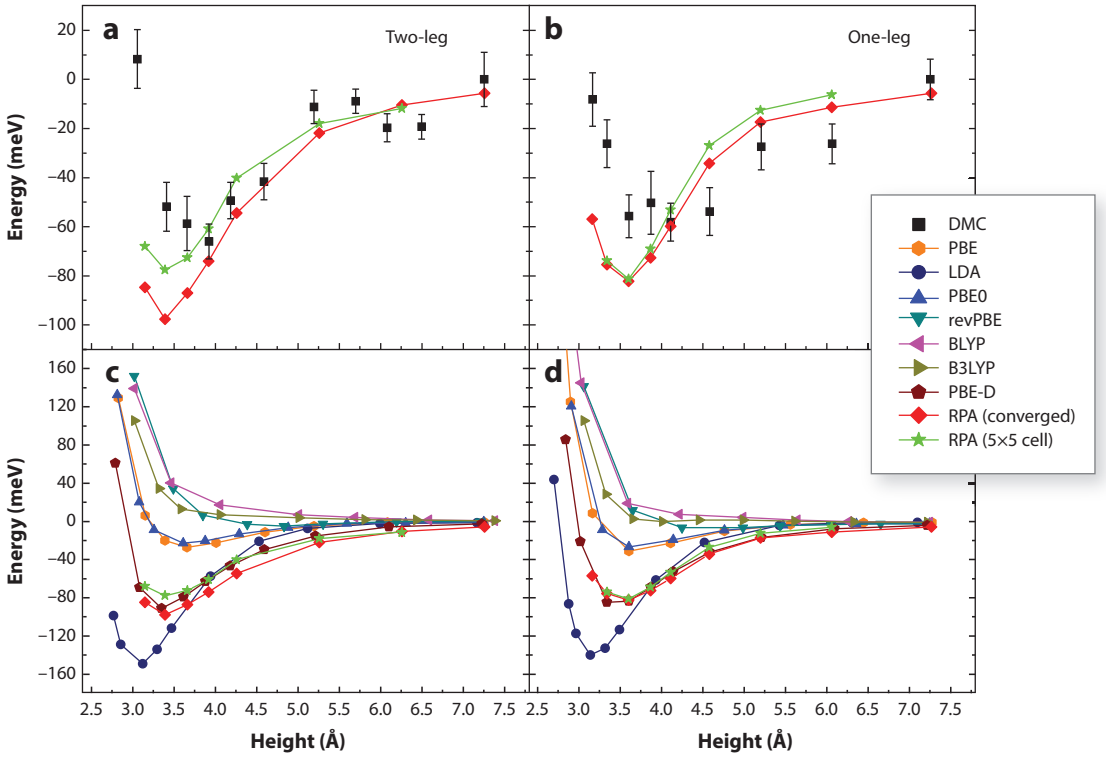

Figure 4

Adsorption energy versus O atom height for a single water molecule on graphene obtained with various ab initio electronic structure–based methods. (*a*,*c*) A so-called two-leg configuration in which both hydrogens of the water molecule are directed at the surface. (*b*,*d*) A so-called one-leg configuration in which only one OH bond is directed at the surface. *a* and *b* compare the accurate reference methods of diffusion quantum Monte Carlo (DMC) and the random phase approximation (RPA). *c* and *d* compare RPA and various forms of density functional theory [i.e., different exchange-correlation functionals: local density approximation (LDA), generalized gradient approximation (BLYP, PBE, and revPBE), hybrid (B3LYP and PBE0), and dispersion-corrected (PBE-D) functionals]. Figure reprinted with permission from Reference 146, ©2011 by the American Physical Society.

interested reader is referred to Reference 169. The limits of DFT for the description of pure water, related to the use of an approximate xc functional, apply also to salt solutions. Bankura et al. (170) recently showed that hybrid functionals (i.e., with the addition of a fraction of exact exchange) that also account for van der Waals forces can provide excellent agreement with experiments for both the structure and electronic properties of a chloride ion solvated in water. Although hybrid functionals are very demanding (computing times are at least an order of magnitude larger than standard semilocal xc functionals), these results are very encouraging concerning the accurate description of both structure and dynamics of aqueous salt solutions. For instance, Li et al. (171) recently used AIMD to explore the mechanisms of selective ion transport in hydrophobic nanochannels, including CNTs (using a standard semilocal functional). They showed that CNTs of suitable size provide very selective ion channels. Such predictions depend strongly on the accuracy of the description of the hydrated ion structure and dynamics, for which AIMD generally proves to be accurate. To illustrate the importance of appropriately describing carbon-water interactions, we refer to a recent manuscript, which discussed the possible reasons why the presence of cations could block water flow through narrow CNTs (172). The authors

used DFT to improve the force fields employed in classical MD simulations. Their results suggest that specific attractions can arise between cations and the aromatic rings located at the opening of (6,6) single-walled CNTs, which can block the pores to water. Perhaps these effects could explain why water permeability through CNT membranes was reported to decay after some time (29).

Finally, we note that although DFT simulations of water/carbon interfaces are not problem free, they can a priori account for water dissociation and polarizability effects. Because both of these issues represent major challenges for traditional force field approaches, with the improvements in the DFT description of van der Waals forces and with the great advances in computing power and algorithmic efficiencies, it seems inevitable that DFT will become increasingly useful in tackling wet carbonaceous interfaces.

Algorithms and Sampling Techniques

Typically in a simulation of a solid-liquid interface, thermostats will be applied to control the temperature of the system. Considerable research goes into thermostat development (see, e.g., Reference 173). We note that, generally, the thermostat implemented can alter the dynamics of the system, to some extent, and so this important technical issue deserves some comment. Thomas & Corry (174) explicitly considered the effect of various algorithms, commonly used to control the temperature in MD simulations, on the predicted water flux across CNT membranes. They considered two groups of algorithms. In the first group, the molecular velocities are rescaled at regular intervals to maintain the effective system temperature within the desired target (e.g., the Berendsen thermostat). In the second group, the molecular velocities are randomized rather than scaled (e.g., the Andersen thermostat). The results showed that the fluxes of water molecules across individual (10,10) CNTs for a given pressure drop significantly depend on the thermostat (direct rescaling yields a flux three times as large as that obtained using a Langevin thermostat, all other system parameters being equal). Thomas & Corry also investigated the permeability as a function of the membrane thickness and found that the results do not show much reduced permeability when velocity-rescaling algorithms are applied, while randomized velocity algorithms lead to decreases in permeability with membrane thickness. As discussed in the section on Carbon Nanotube–Based Membranes, water flow through nanometric CNTs is limited by entrance viscous dissipation (31, 34) and should not depend on tube length for the short tubes considered in the study by Thomas & Corry (37). Therefore, only the velocity rescaling algorithms reproduce the expected behavior. However, this does not mean that randomized velocity algorithms are fundamentally flawed. For instance, Joly studied capillary filling of CNTs with water and obtained consistent results when he compared two different thermostating algorithms; Nosé-Hoover applied only to the degrees of freedom perpendicular to the flow and a dissipative particle dynamics thermostat (34). This thermostat, very similar to the Langevin thermostat, preserves hydrodynamics by construction, as the friction force is proportional to the velocity difference between neighbor atoms, so that it could provide an interesting way to thermostat liquids in complex 3D flows. Overall, these observations should be taken into consideration when insights from simulations are used to interpret experiments. It should also be remembered that it is not clear which algorithms yield the most realistic results, as a direct comparison against experimental data on single CNTs is not yet possible.

Regarding the choice of algorithms to investigate molecular phenomena related to CD applications, it is common practice to apply a uniform charge density on graphitic materials to replicate an applied potential (126, 128, 129). However, this might not always be a realistic representation of the processes. Merlet et al. (175, 176) showed that it is possible to conduct simulations by imposing a constant potential across the simulation cell instead. The distribution of ions within the cell depended on the algorithm applied, especially at high surface charge density. Although

the algorithm is not expected to affect the results at moderate surface charge densities, such as 0.26 e/nm^2, one should be careful in securing reliable connections with experiments when high potentials are considered.

Description of the Material

Computer simulations inevitably involve simplified and very often idealized models of the system under study. Therefore, simulation studies are best suited to better understanding the mechanisms responsible for and underlying physical principles of experimental observations. In such cases, one does not need to replicate the features of an entire RO membrane or CD device. However, it is becoming increasingly important to be able to directly apply the simulations to experiments while reproducing as many features as possible. This is key, e.g., to helping settle arguments such as the large variations reported in water fluxes through CNT-based RO membranes (discussed in the section on Carbon Nanotube–Based Membranes). Gubbins and coworkers (177, 178) developed advanced algorithms for reproducing the subnanometer-level features of carbon adsorbents. Similar approaches should be attempted to replicate the physical properties of GO stacks used in RO membranes, to better understand how processing conditions determine the performance of such devices. Promising results have been obtained when similar approaches were applied to describe the structural evolution of the electrodes used in EDLCs (179), for example. For the applications discussed in this review, it will also be necessary to include a detailed description of the type, density, and distribution of defects, including oxygenated sites and vacancies, that are found in the carbon-based substrates, as these are likely to affect the performance of both RO membranes and CD devices. Once a realistic description of the materials used for water desalination is available, multiscale models, not discussed within this review, will perhaps become useful for discovering new water desalination processes.

Finiteness of Computational Resources

Although computing power continues to rapidly increase with the development of new computing architectures, predictions from simulations likely will always come with uncertainties. With this in mind, it is highly desirable to develop procedures that quantify the propagation of uncertainty from force fields to predicted properties. Angelikopoulos et al. (180) proposed one such approach, based on the Bayesian framework. The authors developed a high-performance computing algorithm for propagating the uncertainties. The approach can be used to estimate simulation model parameters from available experimental data, and also to compare the relative uncertainties of computational predictions, owing to both force fields and algorithms and experimental observables. The development of machine learning potentials, which come with explicit error estimates, also looks like a very promising and powerful avenue for research in this area, especially given the relentless increases in computational power and data storage capacity we are witnessing (181, 182).

CONCLUSIONS

We have reviewed some recent experiments and computational contributions related to the water-energy nexus and, in particular, water desalination. Emphasis was given to membranes for RO and devices for CD. These technologies are leading to the development of increasingly structured nanoporous carbon-based materials. Therefore, understanding at the fundamental level of how water and ions behave in contact with carbon substrates is critical, as is quantifying how external fields and the presence of defects such as oxygenated sites and impurities affect this behavior.

Although considerable insights can be achieved from qualitative comparison between experimental observations and simulations, to truly impact the field we believe that more robust connections between experimental devices and computational approaches are needed. We have discussed some possible ways in which this can be achieved, including experimental observations for single-pore systems and more reliable force fields built with insights from DFT, as well as DFT and beyond-DFT approaches. Although ab initio techniques are extremely versatile, empirical approaches remain useful for studying large systems. We anticipate that multiscale approaches, not discussed here, will become critical for better understanding devices such as GO stacks used in reverse osmosis.

Many open questions remain to be addressed: Why does the water flow through CNT-based membranes quickly stop? If clogging is the culprit, how can we design processes to clean a sub-nanometer pore? How can simulations provide insights to improve the mechanical strength and the resistance to degradation of membranes for water desalination? And, still, what is the true interaction strength between water and carbonaceous surfaces? Surely, a synergistic approach that combines multiscale simulations and experiments can help to address these questions as well. It is also highly probable that new 2D materials beyond carbon will become useful for the water-energy nexus (183). In particular, much emphasis is currently being given to understanding and quantifying the material properties of hexagonal boron nitride and transition metal dichalcogenide monolayers. Perhaps the insights gleaned from carbon-based materials and devices can be helpful in understanding and screening these and other materials.

DISCLOSURE STATEMENT

The authors are not aware of any affiliations, memberships, funding, or financial holdings that might be perceived as affecting the objectivity of this review.

ACKNOWLEDGMENTS

A.S. acknowledges financial support generously provided by the US Department of Energy, the Marie Curie Career Integration Grant, the European Union Horizon 2020 Research and Innovation Program under research grant 640979, the UK Engineering and Physical Sciences Research Council, and Halliburton. A.S. is grateful to his group members for their contribution to the research summarized here, in particular to Dr. Tuan A. Ho, Dr. Dimitrios Argyris, Dr. N.R. Tummala, and Ms. Anh Phan. A.M. is supported by the European Research Council under the European Union's Seventh Framework Program (FP/2007-2013)/ERC Grant Agreement number 616121 (HeteroIce project). A.M. is also supported by the Royal Society through a Royal Society Wolfson Research Merit Award. L.J. is supported by the French Ministry of Defense through the project DGA ERE number 2013.60.0013, and by the LABEX iMUST (ANR-10-LABX-0064) of Université de Lyon, within the program "Investissements d'Avenir" (ANR-11-IDEX-0007) operated by the French National Research Agency (ANR).

LITERATURE CITED

1. Stover RL. 2007. Seawater reverse osmosis with isobaric energy recovery devices. *Desalination* 203:168–75
2. Ghaffour N, Missimer TM, Amy GL. 2013. Technical review and evaluation of the economics of water desalination: current and future challenges for better water supply sustainability. *Desalination* 309:197–207
3. Fritzmann C, Lowenberg J, Wintgens T, Melin T. 2007. State-of-the-art of reverse osmosis desalination. *Desalination* 216:1–76

4. Semiat R. 2008. Energy issues in desalination processes. *Environ. Sci. Technol.* 42:8193–201
5. Elimelech M, Phillip WA. 2011. The future of seawater desalination: energy, technology, and the environment. *Science* 333:712–17
6. Lee KP, Arnot TC, Mattia D. 2011. A review of reverse osmosis membrane materials for desalination—development to date and future potential. *J. Membr. Sci.* 370:1–22
7. Cohen-Tanugi D, Grossman JC. 2015. Nanoporous graphene as a reverse osmosis membrane: recent insights from theory and simulation. *Desalination* 366:59–70
8. Subramani A, Jacangelo JG. 2015. Emerging desalination technologies for water treatment: a critical review. *Water Res.* 75:164–87
9. Daer S, Kharraz J, Giwa A, Hasan SW. 2015. Recent applications of nanomaterials in water desalination: a critical review and future opportunities. *Desalination* 367:37–48
10. Das R, Ali ME, Abd Hamid SB, Ramakrishna S, Chowdhury ZZ. 2014. Carbon nanotube membranes for water purification: a bright future in water desalination. *Desalination* 336:97–109
11. Rodríguez-Calvo A, Silva-Castro GA, Osorio F, González-López J, Calvo C. 2014. Novel membrane materials for reverse osmosis desalination. *Hydrol. Curr. Res.* 5:1–7
12. Müller EA. 2013. Purification of water through nanoporous carbon membranes: a molecular simulation viewpoint. *Curr. Opin. Chem. Eng.* 2:223–28
13. Guo S, Meshot ER, Kuykendall T, Cabrini S, Fornasiero F. 2015. Nanofluidic transport through isolated carbon nanotube channels: advances, controversies, and challenges. *Adv. Mater.* 27:5726–37
14. Kannam SK, Todd BD, Hansen JS, Daivis PJ. 2013. How fast does water flow in carbon nanotubes? *J. Chem. Phys.* 138:094701
15. Park HG, Jung Y. 2014. Carbon nanofluidics of rapid water transport for energy applications. *Chem. Soc. Rev.* 43:565–76
16. Thomas M, Corry B, Hilder TA. 2014. What have we learnt about the mechanisms of rapid water transport, ion rejection and selectivity in nanopores from molecular simulation? *Small* 10:1453–65
17. Ebro H, Kim YM, Kim JH. 2013. Molecular dynamics simulations in membrane-based water treatment processes: a systematic overview. *J. Membr. Sci.* 438:112–25
18. Bocquet L, Charlaix E. 2010. Nanofluidics, from bulk to interfaces. *Chem. Soc. Rev.* 39:1073–95
19. Hummer G, Rasaiah JC, Noworyta JP. 2001. Water conduction through the hydrophobic channel of a carbon nanotube. *Nature* 414:188–90
20. Kalra A, Garde S, Hummer G. 2003. Osmotic water transport through carbon nanotube membranes. *PNAS* 100:10175–80
21. Pascal TA, Goddard WA, Jung Y. 2011. Entropy and the driving force for the filling of carbon nanotubes with water. *PNAS* 108:11794–98
22. Alexiadis A, Kassinos S. 2008. Molecular simulation of water in carbon nanotubes. *Chem. Rev.* 108:5014–34
23. Striolo A. 2006. The mechanism of water diffusion in narrow carbon nanotubes. *Nano Lett.* 6:633–39
24. Falk K, Sedlmeier F, Joly L, Netz RR, Bocquet L. 2010. Molecular origin of fast water transport in carbon nanotube membranes: superlubricity versus curvature dependent friction. *Nano Lett.* 10:4067–73
25. Falk K, Sedlmeier F, Joly L, Netz RR, Bocquet L. 2012. Ultralow liquid/solid friction in carbon nanotubes: comprehensive theory for alcohols, alkanes, OMCTS, and water. *Langmuir* 28:14261–72
26. Joseph S, Aluru NR. 2008. Why are carbon nanotubes fast transporters of water? *Nano Lett.* 8:452–58
27. Striolo A. 2007. Water self-diffusion through narrow oxygenated carbon nanotubes. *Nanotechnology* 18:475704
28. He ZJ, Corry B, Lu XH, Zhou J. 2014. A mechanical nanogate based on a carbon nanotube for reversible control of ion conduction. *Nanoscale* 6:3686–94
29. Majumder M, Chopra N, Andrews R, Hinds BJ. 2005. Nanoscale hydrodynamics: enhanced flow in carbon nanotubes. *Nature* 438:44
30. Deleted in proof.
31. Sisan TB, Lichter S. 2011. The end of nanochannels. *Microfluid. Nanofluid.* 11:787–91
32. Holt JK, Park HG, Wang YM, Stadermann M, Artyukhin AB, et al. 2006. Fast mass transport through sub-2-nanometer carbon nanotubes. *Science* 312:1034–37

33. Qin XC, Yuan QZ, Zhao YP, Xie SB, Liu ZF. 2011. Measurement of the rate of water translocation through carbon nanotubes. *Nano Lett.* 11:2173–77
34. Joly L. 2011. Capillary filling with giant liquid/solid slip: dynamics of water uptake by carbon nanotubes. *J. Chem. Phys.* 135:214705
35. Gravelle S, Joly L, Detcheverry F, Ybert C, Cottin-Bizonne C, Bocquet L. 2013. Optimizing water permeability through the hourglass shape of aquaporins. *PNAS* 110:16367–72
36. Gravelle S, Joly L, Ybert C, Bocquet L. 2014. Large permeabilities of hourglass nanopores: from hydrodynamics to single file transport. *J. Chem. Phys.* 141:18C526
37. Walther JH, Ritos K, Cruz-Chu ER, Megaridis CM, Koumoutsakos P. 2013. Barriers to superfast water transport in carbon nanotube membranes. *Nano Lett.* 13:1910–14
38. Thomas JA, McGaughey AJH. 2009. Water flow in carbon nanotubes: transition to subcontinuum transport. *Phys. Rev. Lett.* 102:184502
39. Majumder M, Chopra N, Hinds BJ. 2011. Mass transport through carbon nanotube membranes in three different regimes: ionic diffusion and gas and liquid flow. *ACS Nano* 5:3867–77
40. Thomas M, Jayatilaka D, Corry B. 2013. How does overcoordination create ion selectivity? *Biophys. Chem.* 172:37–42
41. Sharma S, Debenedetti PG. 2012. Evaporation rate of water in hydrophobic confinement. *PNAS* 109:4365–70
42. Suk ME, Aluru NR. 2013. Molecular and continuum hydrodynamics in graphene nanopores. *RSC Adv.* 3:9365–72
43. Suk ME, Aluru NR. 2014. Ion transport in sub-5-nm graphene nanopores. *J. Chem. Phys.* 140:084707
44. Cohen-Tanugi D, Grossman JC. 2012. Water desalination across nanoporous graphene. *Nano Lett.* 12:3602–8
45. O'Hern SC, Jang D, Bose S, Idrobo JC, Song Y, et al. 2015. Nanofiltration across defect-sealed nanoporous monolayer graphene. *Nano Lett.* 15:3254–60
46. Konatham D, Yu J, Ho TA, Striolo A. 2013. Simulation insights for graphene-based water desalination membranes. *Langmuir* 29:11884–97
47. O'Hern SC, Boutilier MSH, Idrobo JC, Song Y, Kong J, et al. 2014. Selective ionic transport through tunable subnanometer pores in single-layer graphene membranes. *Nano Lett.* 14:1234–41
48. Pendergast MM, Hoek EMV. 2011. A review of water treatment membrane nanotechnologies. *Energ. Environ. Sci.* 4:1946–71
49. Koenig SP, Wang LD, Pellegrino J, Bunch JS. 2012. Selective molecular sieving through porous graphene. *Nat. Nanotechnol.* 7:728–32
50. Garaj S, Hubbard W, Reina A, Kong J, Branton D, Golovchenko JA. 2010. Graphene as a subnanometre trans-electrode membrane. *Nature* 467:190–93
51. Garaj S, Liu S, Golovchenko JA, Branton D. 2013. Molecule-hugging graphene nanopores. *PNAS* 110:12192–96
52. Merchant CA, Healy K, Wanunu M, Ray V, Peterman N, et al. 2010. DNA translocation through graphene nanopores. *Nano Lett.* 10:2915–21
53. Nair RR, Wu HA, Jayaram PN, Grigorieva IV, Geim AK. 2012. Unimpeded permeation of water through helium-leak-tight graphene-based membranes. *Science* 335:442–44
54. Dikin DA, Stankovich S, Zimney EJ, Piner RD, Dommett GHB, et al. 2007. Preparation and characterization of graphene oxide paper. *Nature* 448:457–60
55. Eda G, Chhowalla M. 2010. Chemically derived graphene oxide: towards large-area thin-film electronics and optoelectronics. *Adv. Mater.* 22:2392–415
56. Kim HW, Yoon HW, Yoon SM, Yoo BM, Ahn BK, et al. 2013. Selective gas transport through few-layered graphene and graphene oxide membranes. *Science* 342:91–95
57. Park HB. 2014. Graphene-based membranes—a new opportunity for CO_2 separation. *Carbon Manag.* 5:251–53
58. Li H, Song ZN, Zhang XJ, Huang Y, Li SG, et al. 2013. Ultrathin, molecular-sieving graphene oxide membranes for selective hydrogen separation. *Science* 342:95–98
59. Han Y, Xu Z, Gao C. 2013. Ultrathin graphene nanofiltration membrane for water purification. *Adv. Funct. Mater.* 23:3693–700

60. Sun PZ, Zhu M, Wang KL, Zhong ML, Wei JQ, et al. 2013. Selective ion penetration of graphene oxide membranes. *ACS Nano* 7:428–37
61. Hu M, Mi BX. 2013. Enabling graphene oxide nanosheets as water separation membranes. *Environ. Sci. Technol.* 47:3715–23
62. Huang HB, Mao YY, Ying YL, Liu Y, Sun LW, Peng XS. 2013. Salt concentration, pH and pressure controlled separation of small molecules through lamellar graphene oxide membranes. *Chem. Commun.* 49:5963–65
63. Joshi RK, Carbone P, Wang FC, Kravets VG, Su Y, et al. 2014. Precise and ultrafast molecular sieving through graphene oxide membranes. *Science* 343:752–54
64. Huang LL, Zhang LZ, Shao Q, Wang J, Lu LH, et al. 2006. Molecular dynamics simulation study of the structural characteristics of water molecules confined in functionalized carbon nanotubes. *J. Phys. Chem. B* 110:25761–68
65. Diallo SO, Vlcek L, Mamontov E, Keum JK, Chen JH, et al. 2015. Translational diffusion of water inside hydrophobic carbon micropores studied by neutron spectroscopy and molecular dynamics simulation. *Phys. Rev. E* 91:022124
66. Marti J, Gordillo MC. 2003. Structure and dynamics of liquid water adsorbed on the external walls of carbon nanotubes. *J. Chem. Phys.* 119:12540–46
67. Striolo A, Chialvo AA, Cummings PT, Gubbins KE. 2003. Water adsorption in carbon-slit nanopores. *Langmuir* 19:8583–91
68. Striolo A, Gubbins KE, Gruszkiewicz MS, Cole DR, Simonson JM, Chialvo AA. 2005. Effect of temperature on the adsorption of water in porous carbons. *Langmuir* 21:9457–67
69. Chandler D. 2005. Interfaces and the driving force of hydrophobic assembly. *Nature* 437:640–47
70. Kauzmann W. 1959. Some factors in the interpretation of protein denaturation. *Adv. Protein Chem.* 14:1–63
71. Stillinger FH. 1973. Structure in aqueous solutions of nonpolar solutes from the standpoint of scaled-particle theory. *J. Solut. Chem.* 2:141–58
72. Lum K, Chandler D, Weeks JD. 1999. Hydrophobicity at small and large length scales. *J. Phys. Chem. B* 103:4570–77
73. Huang X, Margulis CJ, Berne BJ. 2003. Dewetting-induced collapse of hydrophobic particles. *PNAS* 100:11953–58
74. Cerdeirina CA, Debenedetti PG, Rossky PJ, Giovambattista N. 2011. Evaporation length scales of confined water and some common organic liquids. *J. Phys. Chem. Lett.* 2:1000–3
75. Altabet YE, Debenedetti PG. 2014. The role of material flexibility on the drying transition of water between hydrophobic objects: a thermodynamic analysis. *J. Chem. Phys.* 141:18C531
76. Remsing RC, Xi E, Vembanur S, Sharma S, Debenedetti PG, et al. 2015. Pathways to dewetting in hydrophobic confinement. *PNAS* 112:8181–86
77. Bakli C, Chakraborty S. 2013. Effect of presence of salt on the dynamics of water in uncharged nanochannels. *J. Chem. Phys.* 138:054504
78. Barrat JL, Bocquet L. 1999. Influence of wetting properties on hydrodynamic boundary conditions at a fluid/solid interface. *Faraday Discuss.* 112:119–27
79. Bakli C, Chakraborty S. 2015. Electrokinetic energy conversion in nanofluidic channels: addressing the loose ends in nanodevice efficiency. *Electrophoresis* 36:675–81
80. Joly L, Ybert C, Trizac E, Bocquet L. 2006. Liquid friction on charged surfaces: from hydrodynamic slippage to electrokinetics. *J. Chem. Phys.* 125:204716
81. Ho TA, Papavassiliou DV, Lee LL, Striolo A. 2011. Liquid water can slip on a hydrophilic surface. *PNAS* 108:16170–75
82. Tocci G, Joly L, Michaelides A. 2014. Friction of water on graphene and hexagonal boron nitride from ab initio methods: very different slippage despite very similar interface structures. *Nano Lett.* 14:6872–77
83. Bocquet L, Barrat JL. 1994. Hydrodynamic boundary-conditions, correlation-functions, and Kubo relations for confined fluids. *Phys. Rev. E* 49:3079–92
84. Bocquet L, Barrat JL. 2013. On the Green-Kubo relationship for the liquid-solid friction coefficient. *J. Chem. Phys.* 139:044704

85. Willard AP, Chandler D. 2009. Coarse-grained modeling of the interface between water and heterogeneous surfaces. *Faraday Discuss.* 141:209–20
86. Acharya H, Vembanur S, Jamadagni SN, Garde S. 2010. Mapping hydrophobicity at the nanoscale: applications to heterogeneous surfaces and proteins. *Faraday Discuss.* 146:353–65
87. Giovambattista N, Lopez CF, Rossky PJ, Debenedetti PG. 2008. Hydrophobicity of protein surfaces: separating geometry from chemistry. *PNAS* 105:2274–79
88. Giovambattista N, Rossky PJ, Debenedetti PG. 2009. Effect of temperature on the structure and phase behavior of water confined by hydrophobic, hydrophilic, and heterogeneous surfaces. *J. Phys. Chem. B* 113:13723–34
89. Hua L, Zangi R, Berne BJ. 2009. Hydrophobic interactions and dewetting between plates with hydrophobic and hydrophilic domains. *J. Phys. Chem. C* 113:5244–53
89a. Striolo A, Chialvo AA, Gubbins KE, Cummings PT. 2006. Simulated water adsorption in chemically heterogeneous carbon nanotubes. *J. Chem. Phys.* 124:074710
90. Gadaleta A, Biance AL, Siria A, Bocquet L. 2015. Ultra-sensitive flow measurement in individual nanopores through pressure-driven particle translocation. *Nanoscale* 7:7965–70
91. Lee CY, Choi W, Han JH, Strano MS. 2010. Coherence resonance in a single-walled carbon nanotube ion channel. *Science* 329:1320–24
92. Christenson HK. 2001. Confinement effects on freezing and melting. *J. Phys. Condens. Matter* 13:R95–R133
93. Majumder M, Zhan X, Andrews R, Hinds BJ. 2007. Voltage gated carbon nanotube membranes. *Langmuir* 23:8624–31
94. Reina A, Thiele S, Jia XT, Bhaviripudi S, Dresselhaus MS, et al. 2009. Growth of large-area single- and bi-layer graphene by controlled carbon precipitation on polycrystalline Ni surfaces. *Nano Res.* 2:509–16
95. Reina A, Jia XT, Ho J, Nezich D, Son HB, et al. 2009. Large area, few-layer graphene films on arbitrary substrates by chemical vapor deposition. *Nano Lett.* 9:30–35
96. Werder T, Walther JH, Jaffe RL, Halicioglu T, Koumoutsakos P. 2003. On the water-carbon interaction for use in molecular dynamics simulations of graphite and carbon nanotubes. *J. Phys. Chem. B* 107:1345–52
97. Hall JE. 1975. Access resistance of a small circular pore. *J. Gen. Physiol.* 66:531–32
98. Greenlee LF, Lawler DF, Freeman BD, Marrot B, Moulin P. 2009. Reverse osmosis desalination: water sources, technology, and today's challenges. *Water Res.* 43:2317–48
99. Busch M, Mickols WE. 2004. Reducing energy consumption in seawater desalination. *Desalination* 165:299–312
100. Lin SH, Elimelech M. 2015. Staged reverse osmosis operation: configurations, energy efficiency, and application potential. *Desalination* 366:9–14
101. Cohen-Tanugi D, McGovern RK, Dave SH, Lienhard JH, Grossman JC. 2014. Quantifying the potential of ultra-permeable membranes for water desalination. *Energ. Environ. Sci.* 7:1134–41
102. Gu MH, Vegas AJ, Anderson DG, Langer RS, Kilduff JE, Belfort G. 2013. Combinatorial synthesis with high throughput discovery of protein-resistant membrane surfaces. *Biomaterials* 34:6133–38
103. Imbrogno J, Williams MD, Belfort G. 2015. A new combinatorial method for synthesizing, screening, and discovering antifouling surface chemistries. *ACS Appl. Mater. Interfaces* 7:2385–92
104. Hansen CM. 2007. *Hansen Solubility Parameters: A User's Handbook*. Boca Raton, FL: Taylor & Francis Group, LLC. 2nd ed.
105. Kwan SE, Bar-Zeev E, Elimelech M. 2015. Biofouling in forward osmosis and reverse osmosis: measurements and mechanisms. *J. Membr. Sci.* 493:703–8
106. Striolo A. 2011. From interfacial water to macroscopic observables: a review. *Adsorpt. Sci. Technol.* 29:211–58
107. Striolo A. 2014. Understanding interfacial water and its role in practical applications using molecular simulations. *MRS Bull.* 39:1062–68
108. Patel AJ, Varilly P, Jamadagni SN, Acharya H, Garde S, Chandler D. 2011. Extended surfaces modulate hydrophobic interactions of neighboring solutes. *PNAS* 108:17678–83
109. Phan A, Cole DR, Striolo A. 2014. Aqueous methane in slit-shaped silica nanopores: high solubility and traces of hydrates. *J. Phys. Chem. C* 118:4860–68

110. Phan A, Cole DR, Striolo A. 2016. Factors governing the behaviour of aqueous methane in narrow pores. *Philos. Trans. R. Soc. A.* 374:50019
111. Oren Y. 2008. Capacitive deionization (CDI) for desalination and water treatment—past, present and future (a review). *Desalination* 228:10–29
112. Anderson MA, Cudero AL, Palma J. 2010. Capacitive deionization as an electrochemical means of saving energy and delivering clean water. Comparison to present desalination practices: Will it compete? *Electrochim. Acta* 55:3845–56
113. Chmiola J, Yushin G, Gogotsi Y, Portet C, Simon P, Taberna PL. 2006. Anomalous increase in carbon capacitance at pore sizes less than 1 nanometer. *Science* 313:1760–63
114. Winter M, Brodd RJ. 2004. What are batteries, fuel cells, and supercapacitors? *Chem. Rev.* 104:4245–69
115. Zhang LL, Zhao XS. 2009. Carbon-based materials as supercapacitor electrodes. *Chem. Soc. Rev.* 38:2520–31
116. Simon P, Gogotsi Y. 2008. Materials for electrochemical capacitors. *Nat. Mater.* 7:845–54
117. Suss ME, Baumann TF, Bourcier WL, Spadaccini CM, Rose KA, et al. 2012. Capacitive desalination with flow-through electrodes. *Energ. Environ. Sci.* 5:9511–19
118. Porada S, Zhao R, van der Wal A, Presser V, Biesheuvel PM. 2013. Review on the science and technology of water desalination by capacitive deionization. *Prog. Mater. Sci.* 58:1388–442
119. Porada S, Sales BB, Hamelers HVM, Biesheuvel PM. 2012. Water desalination with wires. *J. Phys. Chem. Lett.* 3:1613–18
120. Feng GA, Qiao R, Huang JS, Sumpter BG, Meunier V. 2010. Atomistic insight on the charging energetics in subnanometer pore supercapacitors. *J. Phys. Chem. C* 114:18012–16
121. Yang L, Garde S. 2007. Modeling the selective partitioning of cations into negatively charged nanopores in water. *J. Chem. Phys.* 126:084706
122. Shim Y, Kim HJ. 2010. Nanoporous carbon supercapacitors in an ionic liquid: a computer simulation study. *ACS Nano* 4:2345–55
123. Kalluri RK, Konatham D, Striolo A. 2011. Aqueous NaCl solutions within charged carbon-slit pores: partition coefficients and density distributions from molecular dynamics simulations. *J. Phys. Chem. C* 115:13786–95
124. Chialvo AA, Cummings PT. 2011. Aqua ions-graphene interfacial and confinement behavior: insights from isobaric-isothermal molecular dynamics. *J. Phys. Chem. A* 115:5918–27
125. Fedorov MV, Kornyshev AA. 2008. Towards understanding the structure and capacitance of electrical double layer in ionic liquids. *Electrochim. Acta* 53:6835–40
126. Kalluri RK, Biener MM, Suss ME, Merrill MD, Stadermann M, et al. 2013. Unraveling the potential and pore-size dependent capacitance of slit-shaped graphitic carbon pores in aqueous electrolytes. *Phys. Chem. Chem. Phys.* 15:2309–20
127. Kalluri RK, Ho TA, Biener J, Biener MM, Striolo A. 2013. Partition and structure of aqueous NaCl and CaCl2 electrolytes in carbon-slit electrodes. *J. Phys. Chem. C* 117:13609–19
128. Ho TA, Striolo A. 2013. Capacitance enhancement via electrode patterning. *J. Chem. Phys.* 139:204708
129. Ho TA, Striolo A. 2015. Promising performance indicators for water desalination and aqueous capacitors obtained by engineering the electric double layer in nano-structured carbon electrodes. *J. Phys. Chem. C* 119:3331–37
130. Kim S, Lee JK, Kang SO, Ko J, Yum JH, et al. 2006. Molecular engineering of organic sensitizers for solar cell applications. *J. Am. Chem. Soc.* 128:16701–7
131. Ceder G, Chiang YM, Sadoway DR, Aydinol MK, Jang YI, Huang B. 1998. Identification of cathode materials for lithium batteries guided by first-principles calculations. *Nature* 392:694–96
132. Greeley J, Mavrikakis M. 2004. Alloy catalysts designed from first principles. *Nat. Mater.* 3:810–15
133. Studt F, Abild-Pedersen F, Bligaard T, Sorensen RZ, Christensen CH, Norskov JK. 2008. Identification of non-precious metal alloy catalysts for selective hydrogenation of acetylene. *Science* 320:1320–22
134. Vega C, Abascal JLF, Conde MM, Aragones JL. 2009. What ice can teach us about water interactions: a critical comparison of the performance of different water models. *Faraday Discuss.* 141:251–76
135. Babin V, Medders GR, Paesani F. 2012. Toward a universal water model: first principles simulations from the dimer to the liquid phase. *J. Phys. Chem. Lett.* 3:3765–69

136. Ho TA, Striolo A. 2014. Molecular dynamics simulation of the graphene-water interface: comparing water models. *Mol. Simul.* 40:1190–200
137. Liu L, Patey GN. 2014. Simulations of water transport through carbon nanotubes: how different water models influence the conduction rate. *J. Chem. Phys.* 141:18C518
138. Jungwirth P, Tobias DJ. 2002. Ions at the air/water interface. *J. Phys. Chem. B* 106:6361–73
139. Ho TA, Striolo A. 2013. Polarizability effects in molecular dynamics simulations of the graphene-water interface. *J. Chem. Phys.* 138:054117
140. Ma M, Grey F, Shen LM, Urbakh M, Wu S, et al. 2015. Water transport inside carbon nanotubes mediated by phonon-induced oscillating friction. *Nat. Nanotechnol.* 10:692–95
141. Ma M, Tocci G, Michaelides A, Aeppli G. 2016. Fast diffusion of water nanodroplets on graphene. *Nat. Mater.* 15:66–71
142. Carrasco J, Hodgson A, Michaelides A. 2012. A molecular perspective of water at metal interfaces. *Nat. Mater.* 11:667–74
143. Rafiee J, Mi X, Gullapalli H, Thomas AV, Yavari F, et al. 2012. Wetting transparency of graphene. *Nat. Mater.* 11:217–22
144. Li ZT, Wang YJ, Kozbial A, Shenoy G, Zhou F, et al. 2013. Effect of airborne contaminants on the wettability of supported graphene and graphite. *Nat. Mater.* 12:925–31
145. Raj R, Maroo SC, Wang EN. 2013. Wettability of graphene. *Nano Lett.* 13:1509–15
146. Ma J, Michaelides A, Alfe D, Schimka L, Kresse G, Wang EG. 2011. Adsorption and diffusion of water on graphene from first principles. *Phys. Rev. B* 84:033402
147. Chen J, Li XZ, Zhang QF, Michaelides A, Wang EG. 2013. Nature of proton transport in a water-filled carbon nanotube and in liquid water. *Phys. Chem. Chem. Phys.* 15:6344–49
148. Partovi-Azar P, Kühne TD. 2015. Many-body dispersion interactions for periodic systems based on maximally localized Wannier functions: application to graphene/water systems. *Phys. Status Solidi B* 253:308–13
149. Cicero G, Grossman JC, Schwegler E, Gygi F, Galli G. 2008. Water confined in nanotubes and between graphene sheets: a first principle study. *J. Am. Chem. Soc.* 130:1871–78
150. Li X, Feng J, Wang EG, Meng S, Klimes J, Michaelides A. 2012. Influence of water on the electronic structure of metal-supported graphene: insights from van der Waals density functional theory. *Phys. Rev. B* 85:085425
151. Hamada I. 2012. Adsorption of water on graphene: a van der Waals density functional study. *Phys. Rev. B* 86:195436
152. Silvestrelli PL, Ambrosetti A. 2014. Including screening in van der Waals corrected density functional theory calculations: the case of atoms and small molecules physisorbed on graphene. *J. Chem. Phys.* 140:124107
153. McKenzie S, Kang HC. 2014. Squeezing water clusters between graphene sheets: energetics, structure, and intermolecular interactions. *Phys. Chem. Chem. Phys.* 16:26004–15
154. Burke K. 2012. Perspective on density functional theory. *J. Chem. Phys.* 136:150901
155. Gillan MJ, Alfe D, Michaelides A. 2016. Perspective: How good is DFT for water? *J. Chem. Phys.* 144:130901
156. Klimes J, Michaelides A. 2012. Perspective: advances and challenges in treating van der Waals dispersion forces in density functional theory. *J. Chem. Phys.* 137:120901
157. Wu YB, Aluru NR. 2013. Graphitic carbon-water nonbonded interaction parameters. *J. Phys. Chem. B* 117:8802–13
158. Jenness GR, Karalti O, Jordan KD. 2010. Benchmark calculations of water-acene interaction energies: extrapolation to the water-graphene limit and assessment of dispersion-corrected DFT methods. *Phys. Chem. Chem. Phys.* 12:6375–81
159. Jenness GR, Karalti O, Al-Saidi WA, Jordan KD. 2011. Evaluation of theoretical approaches for describing the interaction of water with linear acenes. *J. Phys. Chem. A* 115:5955–64
160. Jenness GR, Jordan KD. 2009. DF-DFT-SAPT investigation of the interaction of a water molecule to coronene and dodecabenzocoronene: implications for the water-graphite interaction. *J. Phys. Chem. C* 113:10242–48

161. Rubes M, Kysilka J, Nachtigall P, Bludsky O. 2010. DFT/CC investigation of physical adsorption on a graphite (0001) surface. *Phys. Chem. Chem. Phys.* 12:6438–44
162. Voloshina E, Usvyat D, Schutz M, Dedkov Y, Paulus B. 2011. On the physisorption of water on graphene: a CCSD(T) study. *Phys. Chem. Chem. Phys.* 13:12041–47
163. Aragones JL, Sanz E, Vega C. 2012. Solubility of NaCl in water by molecular simulation revisited. *J. Chem. Phys.* 136:244505
164. Mester Z, Panagiotopoulos AZ. 2015. Temperature-dependent solubilities and mean ionic activity coefficients of alkali halides in water from molecular dynamics simulations. *J. Chem. Phys.* 143:044505
165. Ding Y, Hassanali AA, Parrinello M. 2014. Anomalous water diffusion in salt solutions. *PNAS* 111:3310–15
166. Kim JS, Wu Z, Morrow AR, Yethiraj A, Yethiraj A. 2012. Self-diffusion and viscosity in electrolyte solutions. *J. Phys. Chem. B* 116:12007–13
167. Jiang H, Mester Z, Moultos OA, Economou IG, Panagiotopoulos AZ. 2015. Thermodynamic and transport properties of H_2O + NaCl from polarizable force fields. *J. Chem. Theory Comput.* 11:3802–10
168. Kiss PT, Baranyai A. 2014. A new polarizable force field for alkali and halide ions. *J. Chem. Phys.* 141:114501
169. Hassanali AA, Cuny J, Verdolino V, Parrinello M. 2014. Aqueous solutions: state of the art in ab initio molecular dynamics. *Philos. Trans. R. Soc. A* 372:20120482
170. Bankura A, Santrab B, DiStasio RA Jr., Swartz CW, Klein ML, Wu X. 2015. A systematic study of chloride ion solvation in water using van der Waals inclusive hybrid density functional theory. *Mol. Phys.* 113:2842–54
171. Li H, Francisco JS, Zeng XC. 2015. Unraveling the mechanism of selective ion transport in hydrophobic subnanometer channels. *PNAS* 112:10851–56
172. Liu J, Shi G, Guo P, Yang J, Fang H. 2015. Blockage of water flow in carbon nanotubes by ions due to interactions between cations and aromatic rings. *Phys. Rev. Lett.* 115:164502(6)
173. Bussi G, Donadio D, Parrinello M. 2007. Canonical sampling through velocity rescaling. *J. Chem. Phys.* 126:014101
174. Thomas M, Corry B. 2015. Thermostat choice significantly influences water flow rates in molecular dynamics studies of carbon nanotubes. *Microfluid. Nanofluid.* 18:41–47
175. Merlet C, Rotenberg B, Madden PA, Taberna PL, Simon P, et al. 2012. On the molecular origin of supercapacitance in nanoporous carbon electrodes. *Nat. Mater.* 11:306–10
176. Merlet C, Pean C, Rotenberg B, Madden PA, Simon P, Salanne M. 2013. Simulating supercapacitors: Can we model electrodes as constant charge surfaces? *J. Phys. Chem. Lett.* 4:264–68
177. Palmer JC, Gubbins KE. 2012. Atomistic models for disordered nanoporous carbons using reactive force fields. *Micropor. Mesopor. Mater.* 154:24–37
178. Jain SK, Pellenq RJM, Pikunic JP, Gubbins KE. 2006. Molecular modeling of porous carbons using the hybrid reverse Monte Carlo method. *Langmuir* 22:9942–48
179. Palmer JC, Llobet A, Yeon SH, Fischer JE, Shi Y, et al. 2010. Modeling the structural evolution of carbide-derived carbons using quenched molecular dynamics. *Carbon* 48:1116–23
180. Angelikopoulos P, Papadimitriou C, Koumoutsakos P. 2012. Bayesian uncertainty quantification and propagation in molecular dynamics simulations: a high performance computing framework. *J. Chem. Phys.* 137:144103
181. Behler J. 2015. Constructing high-dimensional neural network potentials: a tutorial review. *Int. J. Quantum Chem.* 115:1032–50
182. Bartok AP, Csanyi G. 2015. Gaussian approximation potentials: a brief tutorial introduction. *Int. J. Quantum Chem.* 115:1051–57
183. Heiranian M, Farimani AB, Aluru NR. 2015. Water desalination with a single-layer MoS_2 nanopore. *Nat. Commun.* 6:8616

Annual Review of Chemical and Biomolecular Engineering

Volume 7, 2016

Contents

Indexes

Errata

An online log of corrections to *Annual Review of Chemical and Biomolecular Engineering* articles may be found at http://www.annualreviews.org/errata/chembioeng